2001

Value of Incorporating Satellite-Derived Land Cover Data in MM5/PLACE for Simulating Surface Temperatures

Todd M. Crawford
NOAA/National Severe Storms Laboratory, Norman

David J. Stensrud
NOAA/National Severe Storms Laboratory, david.stensrud@nssl.noaa.gov

Franz Mora
University of Nebraska—Lincoln

James W. Merchant
University of Nebraska - Lincoln, jmerchant1@unl.edu

Peter J. Wetzel
NASA Goddard Space Flight Center, Greenbelt

Value of Incorporating Satellite-Derived Land Cover Data in MM5/PLACE for Simulating Surface Temperatures

TODD M. CRAWFORD AND DAVID J. STENSRUD

NOAA/National Severe Storms Laboratory, Norman, Oklahoma

FRANZ MORA AND JAMES W. MERCHANT

Center for Advanced Land Management Information Technologies, University of Nebraska—Lincoln, Lincoln, Nebraska

PETER J. WETZEL

Mesoscale Atmospheric Processes Branch, NASA Goddard Space Flight Center, Greenbelt, Maryland

(Manuscript received 7 June 2000, in final form 5 January 2001)

ABSTRACT

The Parameterization for Land–Atmosphere–Cloud Exchange (PLACE) module is used within the Fifth-Generation Pennsylvania State University–National Center for Atmospheric Research Mesoscale Model (MM5) to determine the importance of individual land surface parameters in simulating surface temperatures. Sensitivity tests indicate that soil moisture and the coverage and thickness of green vegetation [as manifested by the values of fractional green vegetation coverage (fVEG) and leaf area index (LAI)] have a large effect on the magnitudes of surface sensible heat fluxes. The combined influence of LAI and fVEG is larger than the influence of soil moisture on the partitioning of the surface energy budget. Values for fVEG, albedo, and LAI, derived from 1-km-resolution Advanced Very High Resolution Radiometer data, are inserted into PLACE, and changes in model-simulated 1.5-m air temperatures in Oklahoma during July of 1997 are documented. Use of the land cover data provides a clear improvement in afternoon temperature forecasts when compared with model runs with monthly climatological values for each land cover type. However, temperature forecasts from MM5 without PLACE are significantly more accurate than those with PLACE, even when the land cover data are incorporated into the model. When only the temperature observations above 37°C are analyzed, however, the simulations from the high-resolution land cover dataset with PLACE significantly outperform MM5 without PLACE. Previous land surface models have simply used (at best) climatological values of these crucial land cover parameters. The ability to improve model simulations of surface energy fluxes and the resultant temperatures in a diagnostic sense provides promise for future attempts at ingesting satellite-derived land cover data into numerical models. These model improvements would likely be most helpful in predictions of extreme temperature events (during drought or extremely wet conditions) for which current numerical weather prediction models often perform poorly. The potential value of real-time land cover information for model initialization is substantial.

1. Introduction

The importance of land surface characteristics, such as relative amounts of vegetation and bare soil, soil type, surface roughness, and soil moisture, in determining the relative magnitudes of the terms in the surface energy budget has been demonstrated clearly (National Research Council 1991). The interactions between land surface processes and the atmosphere are now widely recognized as being important to both climate change (National Research Council 1991; Pitman et al. 1999) and short-term weather forecasting (Emanuel et al. 1995). As a result, there has been a noticeable increase in the last decade in the number of American Meteorological Society and American Geophysical Union conference papers that examine land–atmosphere interactions (Lawford 1999).

Emanuel et al. (1995) stress the importance of gaining a better understanding of land–atmosphere interactions for applications in numerical modeling and weather forecasting. Lawford (1999), in the midterm report of the Global Energy and Water Cycle Experiment Continental-Scale International Project, further emphasizes the need to understand the role of vegetation in land surface forcing. This is particularly important as many land surface schemes, which include explicit representations of vegetation, are incorporated into meteorological models with spatial resolutions ranging from a few to hundreds of kilometers (e.g., Dickinson et al. 1986;

Corresponding author address: Dr. David J. Stensrud, National Severe Storms Laboratory, 1313 Halley Circle, Norman, OK 73069. E-mail: david.stensrud@nssl.noaa.gov

Noilhan and Planton 1989; Wetzel and Boone 1995; Chen et al. 1996). These schemes are key components in models used for short- and medium-range weather forecasting and global climate change studies.

Previous studies have emphasized the sensitivity of the Bowen ratio (the ratio of the sensible and latent heat fluxes) to various land surface parameters. Sud et al. (1988) conclude that significant variations in surface roughness have little effect on the relative magnitudes of sensible and latent heat fluxes. Dickinson and Henderson-Sellers (1988) conversely find that surface roughness is the most important factor in changes to the surface energy budget. Collins and Avissar (1994) determine that soil moisture, leaf area index, surface roughness, albedo, and plant stomatal conductance are most important in determining the magnitude of the individual surface energy fluxes. Niyogi et al. (1999) show that there are significant nonlinear interactions among the various land surface parameters that cannot be ignored. These results suggest that no single land surface parameter is more important than any other for correctly simulating the surface energy fluxes.

The lack of a few dominant land surface parameters for specifying the correct surface energy fluxes may explain why, even with sophisticated land surface parameterization schemes, significant improvements in meso- and storm-scale numerical weather prediction model low-level temperature forecasts have been relatively slow in developing. Colby (1998) examines output from the current operational forecast models across the entire United States and finds that significant boundary layer temperature errors continue to occur with some regularity. Yet accurate temperature forecasts are particularly important to many industries, such as agriculture, transportation, and power generation, in daily operations (Wilks 1997; Brooks and Douglas 1998; Dempsey et al. 1998). It is possible that some of the difficulties in correctly forecasting surface temperatures may be due to a poor depiction of spatially and temporally varying land surface characteristics.

The land cover characteristics assigned in most mesoscale numerical weather prediction models often are obtained from monthly climatological data (e.g., Dickinson et al. 1986; Noilhan and Planton 1989; Wetzel and Boone 1995; Chen et al. 1996). Monthly data capture the gross seasonal cycle of the vegetation, but important details are masked by this longer time interval. In addition, the use of climatological values also masks seasonal variations in the timing of the emergence and senescence of vegetation that are known to occur across the United States (Schwartz and Karl 1990). Rabin et al. (1990) document that the harvesting of winter wheat in Oklahoma leads to an increase in daily high temperatures of up to 3°C, yet this harvesting occurs over the period of about one week and would not be captured using a monthly vegetation data base. Moreover, the year-to-year variability in the time of the wheat harvest spans several weeks and depends upon both soil conditions and the weather.

These results suggest that use of real-time, or near-real-time, land cover data could lead to significant improvements in the forecasting of temperatures near the ground surface. In recent years, capabilities to inventory and map land cover conditions and to monitor land cover changes at high spatial and temporal resolution using satellite imagery have evolved rapidly. Lawford (1999) suggests that such data must be used more effectively in land–atmosphere parameterizations.

Although earth-observing satellites, such as Landsat and ''SPOT,'' are widely employed for land cover assessment, their utility in weather and climate modeling is limited by several factors. First, because such models demand data covering very large areas, dozens to hundreds of images may be required. The costs of data acquisition and analysis generally make such analyses prohibitively expensive. In addition, the revisit period of most earth-observing satellites (e.g., 16 days for *Landsat-7*) is currently such that high-quality, cloud-free images can be obtained only infrequently over many locations. As a consequence, many scientists interested in characterizing and monitoring land cover over very large areas have, in recent years, turned to meteorological satellite data (Ehrlich et al. 1994). Most research has focused on the Advanced Very High Resolution Radiometer (AVHRR), a sensor carried on the National Oceanic and Atmospheric Administration's polar-orbiting satellites (Ehrlich et al. 1994). AVHRR provides low-cost daily global coverage at approximately 1-km spatial resolution. The high frequency of imaging provides many opportunities for acquisition of cloud-free data over relatively short time periods, enabling one to observe and map short-term changes in land cover. The 1-km spatial resolution produces a manageable volume of data for regional and even global applications.

Most research on land cover characterization using AVHRR data has involved assessment of the normalized difference vegetation index (NDVI), a metric that expresses contrast between reflectance of red light and near-infrared energy, computed as (channel 1 − channel 2)/(channel 1 + channel 2), where channel 1 represents the reflectance of red light and channel 2 represents the reflectance of near-infrared radiation. Multitemporal AVHRR NDVI data have been widely used to map land cover types and the seasonal development of vegetation (Reed and Yang 1997; Loveland et al. 1995) and to estimate a wide variety of biophysical parameters, including primary production, the green vegetation fraction, leaf area index (LAI), and surface albedo (Champeaux et al. 2000; Csiszar and Gutman 1999; Gutman and Ignatov 1998; Yin and Williams 1997; Price 1993; Box et al. 1989). It is usual, in such efforts, to work with composite NDVI images comprising the maximum NDVI value occurring in each 1-km pixel over a 10–14-day composite period. Because high NDVI values are associated with growing vegetation and lower values

are associated with clouds, this procedure tends to produce composite images that are largely cloud free. Biweekly maximum NDVI datasets produced by the United States Geological Survey Earth Resources Observation Systems Data Center are used in this study (Eidenshink and Hutchinson 1993). Previous studies suggest that AVHRR data can be used to provide the initial land cover parameters needed in numerical weather prediction models.

The goal of this study is to explore the value of near-real-time AVHRR-derived land use and land cover information for simulating surface temperatures. In particular, 1-km values of LAI, surface albedo, and fractional green vegetation coverage (fVEG) are derived and inserted into the initial conditions of a mesoscale model. Simulations from these initial conditions are compared with those from climatological data to see if the AVHRR-derived land use and land cover data produce improved simulations of near-surface temperature. If true, then the development of methods to compute these land use and land cover metrics in real time is desirable and warranted. These simulations also are compared with those from a simplified land surface scheme to assess the improvements in surface temperature forecasts from the more sophisticated land surface physics.

The numerical model used in this study is briefly described in section 2. The relative importance of various land surface characteristics is examined through a series of sensitivity tests in section 3. In section 4, the methods by which the AVHRR-derived 1-km values of LAI, surface albedo, and fVEG are incorporated into the numerical model are documented. Model simulations of 1.5-m air temperatures are then compared with observed afternoon temperatures from Oklahoma Mesonet (Brock et al. 1995) and National Weather Service (NWS) stations in section 5 for seven clear days from July of 1997 to document the improvement in model forecasts using this new land cover dataset. A final discussion is found in section 6.

2. Numerical model

The model chosen for use in this study is the nonhydrostatic Fifth-Generation Pennsylvania State University–National Center for Atmospheric Research Mesoscale Model (MM5; Dudhia 1993). MM5 offers numerous user options, including the ability to have multiple grids and to choose from various convective, boundary layer, and cloud physics parameterizations. Either a single grid or a two-way interactive nested grid is used in this study. All domains have 40 vertical sigma levels that are concentrated in the planetary boundary layer to simulate better the development and evolution of the low-level temperature and moisture fields.

Although a convective parameterization scheme and grid-scale microphysics are active in the model runs, the days selected for study are those in which the skies are generally clear and no rainfall is reported over most of the inner model domain. As such, these schemes have little or no influence on the model simulations. In addition, to simplify the comparison of the model surface temperatures from various initial values of land use and land cover, no attenuation of solar radiation by clouds is allowed. In this way, errors in cloud cover are not allowed to influence the simulations, and the downwelling solar radiation at the surface is the same in all the simulations. Any differences in surface temperatures that occur are due to changes in land surface processes.

One of the user-defined options in MM5 is a modified version of the Blackadar (1979) high-resolution planetary boundary layer parameterization scheme (Zhang and Anthes 1982). With this scheme, during typical daytime conditions, mixing occurs between the lowest model level and the entire boundary layer. Because it is unclear how much improvement in surface temperature forecasts is made by upgrading from a simplified land surface scheme to a sophisticated land surface scheme that includes explicitly the effects of vegetation, two very different schemes are used to calculate the surface energy budget.

a. Default scheme

In this scheme, the ground surface temperature is computed following a force–restore slab model (Deardorff 1978; Zhang and Anthes 1982) that explicitly calculates the sensible, latent, and ground heat fluxes that result from partitioning the net available radiation. The soil consists of two layers: a 10-cm-deep layer that interacts directly with the atmosphere and a lower substrate layer that acts as a deep thermal reservior and retains a constant temperature (see Fig. 1). Variability in soil wetness is incorporated indirectly via a moisture availability parameter M, which varies from 0 to 1 and strongly influences the calculation of latent heat flux. The values of M are determined using an antecedent precipitation index (API) that uses 24-h accumulated rainfall data from over 6000 reporting stations within the contiguous United States. The values of M are calculated on a 0.25° latitude and longitude grid and are bilinearly interpolated to all the MM5 grid points. This API technique is described more fully in Chang and Wetzel (1991). Deardorff (1978) finds that a force–restore scheme is superior to five other schemes in computing ground temperature and heat flux. However, the value of M does not influence the soil thermal capacity, and the physical processes of water transport within both the soil and vegetation are ignored.

b. PLACE scheme

To simulate more accurately the effects of vegetation, the Parameterization for Land–Atmosphere–Cloud Exchange (PLACE; Wetzel and Boone 1995) module is used within MM5. PLACE, a seven-layer land surface module, is intended to couple the atmosphere and the

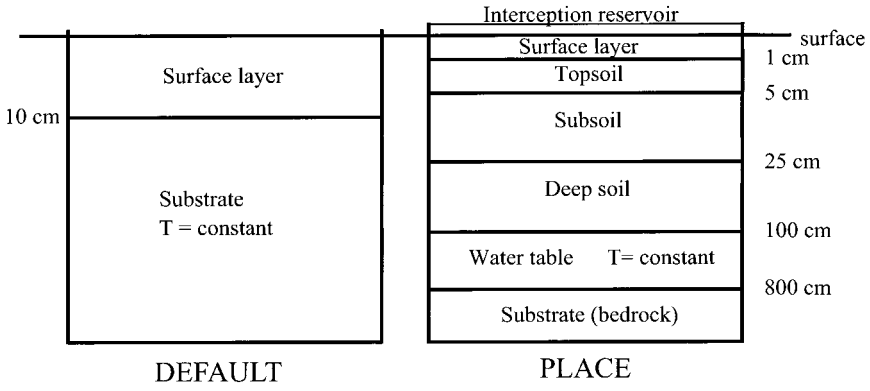

FIG. 1. Schematic comparing the default force–restore land surface scheme with PLACE.

surface in a physically realistic manner through detailed parameterizations of surface energy fluxes and soil water movement. A comparison of the vertical structures of the force–restore and PLACE schemes illustrates the added complexity and detail of PLACE (Fig. 1), which, one hopes, leads to an improved prediction of surface fluxes and temperatures.

When PLACE is used within MM5, the boundary layer scheme provides information about the atmospheric conditions at the lowest model level to PLACE. PLACE then computes the surface energy fluxes and the soil temperatures and moistures, returning these values to the boundary layer scheme. Each model grid cell is treated as having a specified fraction of fully vegetated surface, defined by fVEG, with the remainder of the surface assumed to be nonvegetated bare soil. As described in Wetzel and Boone (1995), separate evapotranspiration equations are used to compute supply- and demand-limited rates for vegetation and bare soil. The demand-limited rate is a function of the mixing-ratio gradient between the ground and the surface layer and of the magnitude of the canopy resistance (Noilhan and Planton 1989). The supply-limited rates are dependent upon the gradient between the water potentials of the soil and plant. The resulting latent heat flux in a grid cell is a weighted sum of the fluxes from the vegetated and bare soil areas within that cell.

The vegetation types used by PLACE are converted from the standard MM5 types. Soil type, roughness length, surface albedo, LAI, and fVEG are based on field observations from the International Satellite Land Surface Climatology Project (ISLSCP; Sellers et al. 1995, 1996) and are dependent upon the PLACE vegetation type. For each vegetation type, a random number generator is used to select the values of these parameters based on the observed ISLSCP distributions. Although it is possible to use other data sources to provide more detailed land surface information, soil and vegetation characteristics can vary widely over short distances. Thus, a stochastic approach is used to initialize PLACE, instead of a more explicit one, to mimic this variability. When the AVHRR-derived values of albedo, LAI, and fVEG are used, these values are inserted directly into the model and replace the default, stochastic distributions determined for PLACE.

The surface energy budget equation is solved at the surface–atmosphere interface. The surface temperature acts as the upper (lower) boundary condition for the calculation of the soil (sensible) heat flux. The soil heat flux is calculated as a function of the vertical temperature gradient between the surface and the top model soil layer and is dependent upon the values of soil thermal conductivity and diffusivity. Sensible heat flux is calculated based upon the temperature gradient between the surface and the lowest model level within the planetary boundary layer and depends upon the values of roughness length and near-surface stability.

Water within PLACE is stored separately as dew, as intercepted precipitation, and as soil moisture in the surface soil, two root zones, and two deeper soil layers. Root fractions are specified as 50% in the topsoil layer, with 25% in each of the two deeper soil layers. Soil moisture is determined using the M values calculated from the API as described by Chang and Wetzel (1991) and also as used in the force–restore land surface scheme. However, for use in PLACE, the values of M are used only to scale linearly between the two specified values of soil moisture (wilting point and field capacity) defined for each soil type. Thus, the values of soil moisture used are linearly dependent upon M and also are assumed to be constant with depth. A comparison between values of M and volumetric water content from the Oklahoma Mesonet during July of 1997 (Crawford et al. 2000, hereinafter CSCC) indicates a Pearson correlation coefficient of 0.76. Thus, the simple API scheme provides a reasonable indication of the horizontal variability in soil moisture. Soil temperatures at each vertical level are specified by adding a random perturbation to the initial values of ground temperature given by MM5.

Results from the Project for Intercomparison of Land Surface Parameterization Schemes indicate that the behavior of PLACE is consistent with other land surface schemes and with field observations (Chen et al. 1997).

Further details on PLACE can be found in Wetzel and Boone (1995).

For each of the model simulations described below, the simulations are started at 1200 UTC and are run out to at least 9 h to capture most of the daytime heating cycle. The atmospheric initial conditions are obtained by using the global analyses from the National Centers for Environmental Prediction as a first-guess field and blending in all standard surface and rawinsonde observations as described by Benjamin and Seaman (1985). Boundary conditions are also determined at a 12-h interval using these data. No special observational datasets are used, in order to mimic what is available to current operational numerical weather prediction models. Before proceeding with an analysis of the observed cases, sensitivity tests are used to illustrate the potential benefits of high-resolution land use and land cover data.

3. Sensitivity tests

To ascertain the sensitivity of MM5–PLACE to several different land surface parameters, simple sensitivity tests are performed. For these initial tests, the model is run using a single 151 × 151 grid at 20-km spacing with a 70-s time step. Monthly climatological values of land cover parameters derived from ISLSCP are used as described above. 12 July 1997 is chosen for testing because it was a clear, synoptically quiescent day across Oklahoma, and the model is started at 1200 UTC and is run out to 0000 UTC 13 July 1997. The instantaneous, hourly modeled fluxes are interpolated bilinearly to 44 specified Oklahoma Mesonet sites for comparative purposes, and the values of sensible heat flux from these locations are averaged to obtain a representative statewide average.

Each of five land surface parameters are artificially increased and decreased by 25%, in turn, to discern their relative importance. Three of these parameters—LAI, fVEG, and albedo—can be estimated directly from AVHRR data. The other two parameters, soil moisture and roughness length, must be determined from other sources. Roughness length depends upon many factors, including vegetation height and density (Monteith and Unsworth 1990), but likely can be estimated from vegetation databases. Soil moisture is likely the most difficult parameter to determine, because it depends not only upon the vegetation and land cover characteristics but also upon the antecedent rainfall and the soil type and texture. Sensitivity to soil texture is not examined here, but Wetzel and Chang (1988) show that changes in soil type and various empirical soil parameters can produce large differences in sensible heat fluxes. The sensitivity of PLACE to each of these five parameters is now examined.

a. Soil moisture

Soil moisture within PLACE is estimated using the default values of M from the standard MM5 land use categories. These default values of M are specified as a function of land use category, have a constant summer value, and are supplied by MM5. CSCC show that a 20% variation in soil volumetric water content represents the root-mean-square error (rmse) one might find in predicting soil moisture over a state-sized region, although errors at specific stations may be much larger. Thus, the 25% variation used in these tests appears reasonable as a guess to the current accuracy of soil moisture predictions. The areal-average sensible heat fluxes H for the different magnitudes of M (insuring that final values are bounded by 0 and 1 and holding all other parameters constant) results in a variation in H of 32% of the default value (Fig. 2a). Smaller (larger) values of M result in larger (smaller) values of H, because less (more) of the available radiative energy is used to produce evapotranspiration from the surface.

b. Surface roughness

Variations in surface roughness values of 25% are easily within the range of uncertainty, because an incorrect vegetation category assignment can result in a much larger difference. As with the values of M, the surface roughness z_0 was also varied from 75% to 125% of the default model-specified value. This range of z_0 results in a variation in H of about 3% of the default value (not shown), a much smaller range than seen for similar percentage changes in soil moisture. Smaller (larger) roughness values are expected to result in smaller (larger) sensible and latent heat flux values, since vertical turbulent momentum fluxes are reduced (increased) and more (less) radiative energy goes into the ground. This result agrees with those of Wetzel and Chang (1988).

c. Leaf area index

Using only 3 yr of LAI values during June and July over the central plains of the United States, as derived from AVHRR data (details provided in the next section), it is estimated that differences in LAI of 25% can occur for the same location, during the same two-week period, from one year to the next. Within PLACE, the values of LAI influence the vegetation canopy resistance, with larger LAI values causing the resistance to decrease. Model results indicate that variations in LAI have a considerable impact on the magnitude of H. Varying the LAI from 75% to 125% of the climatological value results in a variation in H of 28% of the default value (Fig. 2b), nearly as large a variation as seen from changes in soil moisture. Larger (smaller) values of LAI result in smaller (larger) values of H because there is more (less) green, transpiring surface area, thus reducing (increasing) the sensible heat flux.

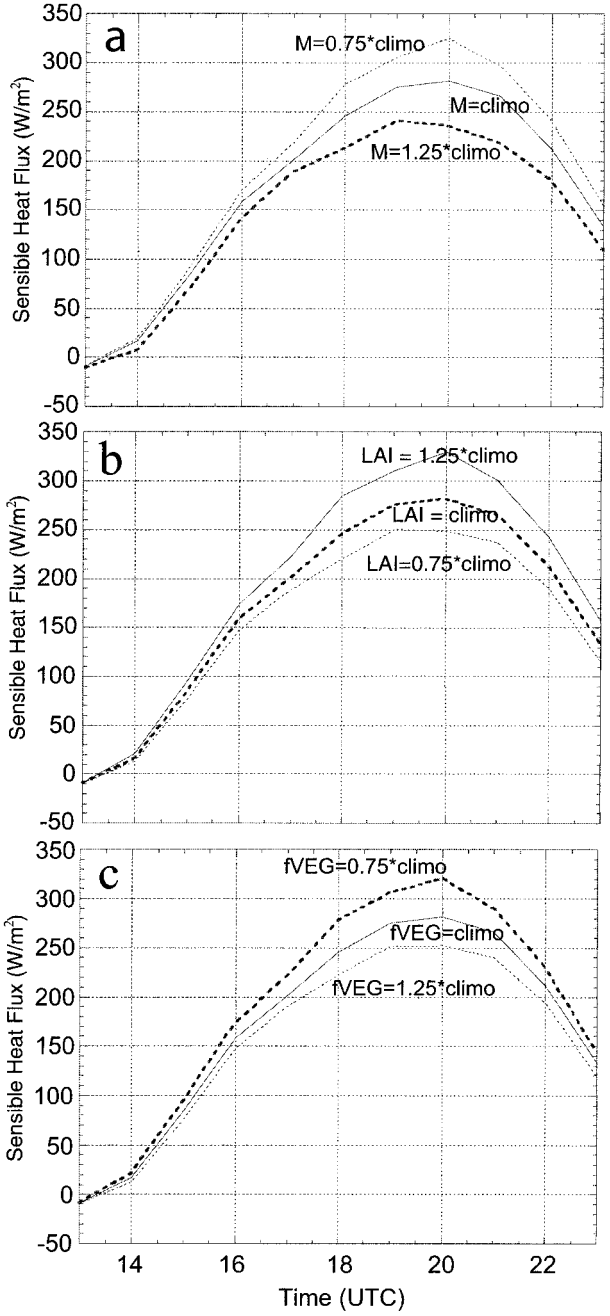

FIG. 2. Sensitivity of model-produced (MM5–PLACE:ISLSCP) hourly, Oklahoma-average sensible heat flux values (W m^{-2}) to changes in (a) *M*, (b) LAI, and (c) fVEG between 1200 UTC 12 Jul and 0000 UTC 13 Jul 1997.

d. Fractional green vegetation coverage

As with the LAI values, differences of 25% in fVEG can easily occur from one year to the next for any given location during the same two-week period. Thus, fVEG is also varied from 75% to 125% percent of the default values, with the requirement that the final values remain between 0 and 1. The maximum variation in *H* across this range of values is approximately 70 W m^{-2}, or 24% (Fig. 2c). Similar to the results from changing the LAI, larger (smaller) values of fVEG result in smaller (larger) values of *H* because there is more (less) surface area covered by green, transpiring vegetation. This also is consistent with the results of Wetzel and Chang (1988).

TABLE 1. Variation in simulated sensible heat flux *H* over Oklahoma when each individual land surface parameter is varied separately from 75% to 125% of its default value.

Land surface parameter	Variation in *H*
Moisture availability (*M*)	32%
Leaf area index (LAI)	28%
Fractional vegetation cover (fVEG)	24%
Albedo	12%
Roughness length (z_0)	3%

e. Surface albedo

The surface albedo is varied from 75% to 125%, again with the requirement that the final values be confined to between 0 and 1. This test results in a relatively small variation in *H* of 12% (not shown). Increases (decreases) in albedo result in less (more) available radiative energy at the surface, which reduces (increases) both sensible and latent heat fluxes.

f. All factors

The relative importance of the five land surface parameters indicates that soil moisture, LAI, and fVEG are most important, followed by albedo and roughness length (Table 1). Other parameters, such as soil type, also may be important. These results mirror those found by Wetzel et al. (1984) and Wetzel and Chang (1988), when testing PLACE in stand-alone mode. To ascertain the largest possible variation in *H* as a result of changes in land surface parameters, the values of z_0 are increased by 25% and the values of *M*, LAI, fVEG, and albedo are all decreased by 25% simultaneously so as to achieve the largest possible increase in *H* (Table 2). In a similar way, the opposite changes are made (values of z_0 are decreased by 25%, and values of *M*, LAI, fVEG, and albedo are increased by 25% simultaneously) so as to

TABLE 2. Variations (W m^{-2}) in *H* when each parameter is varied separately, while holding the others constant, from 75% to 125% of its default value. The bottom row represents the model runs in which all five parameters are varied simultaneously to maximize or minimize *H*.

Land surface parameter	Increase *H*	Decrease *H*
Moisture availability (*M*)	43	46
Leaf area index (LAI)	48	33
Fractional vegetation cover (fVEG)	39	29
Albedo	17	18
Roughness length (z_0)	4	5
Sum	151	131
All five parameters	117	103

achieve the largest possible decrease in *H*. It is apparent that, by adding the changes in *H* for each land surface parameter sensitivity run (Table 2), the sum of the variations found from each of the individual land surface parameters is greater than the actual variation in *H* when all of the parameters are combined. The total variation in *H* when all five parameters are altered simultaneously is 220 W m^{-2}, or about 80% of the potential maximum value. This result supports the notion that there is no single dominant land surface parameter determining the surface energy fluxes and that good estimates of all the land characteristics used in the model are needed to produce good forecasts of surface temperatures.

These sensitivity tests highlight the importance of a proper specification of fVEG and LAI in a land surface model. Because these land cover characteristics are typically defined in atmospheric models by using climatological vegetation datasets, the remainder of this study focuses on inserting AVHRR-derived land cover data into MM5–PLACE and documenting the improved surface temperature simulations that occur when using these data.

4. Retrieval of AVHRR-derived land cover parameters

Four successive AVHRR 14-day maximum NDVI composite images, encompassing in total almost all of June and July of 1997, are used to estimate broadband surface albedo, fVEG, and LAI during the study time period and region. For a given model simulation, the NDVI composite image that contains the particular day of interest is used to determine these three land surface parameters. No interpolation in time is used. Thus, variations that occur within the 14-day sampling interval are ignored. Since all the selected model simulations occur during July, when the land surface conditions typically do not vary as quickly with time over most of the study region, this limitation is reasonable and is not expected to influence the results substantially.

The broadband surface albedo is calculated from the AVHRR data by a narrowband-to-broadband conversion using a linear combination of the individual isotropic albedos of the visible and near-infrared bands as in Wydick et al. (1987). However, the more recent weighting coefficients of Csizar and Gutman (1999) are used.

The values of LAI are calculated assuming a linear relationship between NDVI and LAI as in Zhangshi and Williams (1997), such that

$$\mathrm{LAI}_i = \mathrm{LAI}_{\max}(\mathrm{NDVI}_i - \mathrm{NDVI}_{\min}) \div (\mathrm{NDVI}_{\max} - \mathrm{NDVI}_{\min}) \quad (1)$$

where the subscripts max, min, and *i* refer to the maximum, minimum, and period values observed at a particular location, respectively. The maximum and minimum NDVI values are calculated from annual series of NDVI from 1995–99 over the region of interest and for each data location. The maximum values of LAI are calibrated from 1-km land cover data (Loveland et al. 1995), in which the maximum LAI at a given point is assigned based upon the associated land cover type. Although it is known that there is an asymptotic saturation level of LAI as the values of NDVI increase (Carlson and Ripley 1990), the relation between LAI and NDVI is typically linear for LAI values less than 3.

The values of fVEG are calculated using the two-line-segment method of Chang and Wetzel (1991) in which the linear relationship between fVEG and NDVI changes abruptly as the NDVI value exceeds 0.547. This method provides an optimum fit to field validation data reported by Asrar et al. (1984) and Los et al. (2000), assuming fVEG and the fraction of photosynthetically active radiation (fPAR) are linearly related. These field data, from five intensive satellite validation field experiments, contain considerable scatter (e.g., Los et al. 2000, their Fig. 5a). However, a simple linear relationship between NDVI and fVEG, such as proposed by Gutman and Ignatov (1995), falls well outside the range of the scatter. The linear relationship between fVEG and fPAR is exact if all leaves absorb 100% of radiation in the photosynthetically active range. Because typical leaf absorption is around 95%, the assumption of linearity is very accurate. Because of incomplete cloud screening, aerosol correction, species differences, and many other issues, the observational and theoretical basis for converting satellite NDVI to model input parameters such as fVEG and LAI could benefit greatly from further study.

To aggregate the 1-km land cover data to the model grid, a simple averaging routine is used. Each of the 1-km land cover values (see Fig. 3) is assigned to the closest model grid box, and all the values within a grid box are averaged to get a representative value of LAI, fVEG, and albedo, respectively. Values representing water surfaces are not used in the averaging process. Note that linear averaging of fVEG and LAI does not have the same effect as the linear averaging of albedo. The latter quantity is, to a close approximation, linearly related to the magnitude of the surface energy fluxes it controls. However, the relationship between LAI and the surface fluxes, for example, is nonlinear. Increasing LAI from 1 to 2 has a much greater effect on the sensible and latent heat fluxes than does increasing LAI from 2 to 4.

The differences in the early-July 1997 AVHRR-derived and the ISLSCP July climatological values of fVEG and LAI clearly indicate the variations in land surface characteristics that can occur within a given year (Fig. 4). Differences are as large as 0.44 in fVEG and as large as 6.0 in LAI. Differences approaching or exceeding these magnitudes are also seen when comparing values calculated from a 3-yr average July composite NDVI map with the values from the first two weeks of 1997, which show maximum 1-km grid differences of 0.59 in fVEG and 2.95 in LAI.

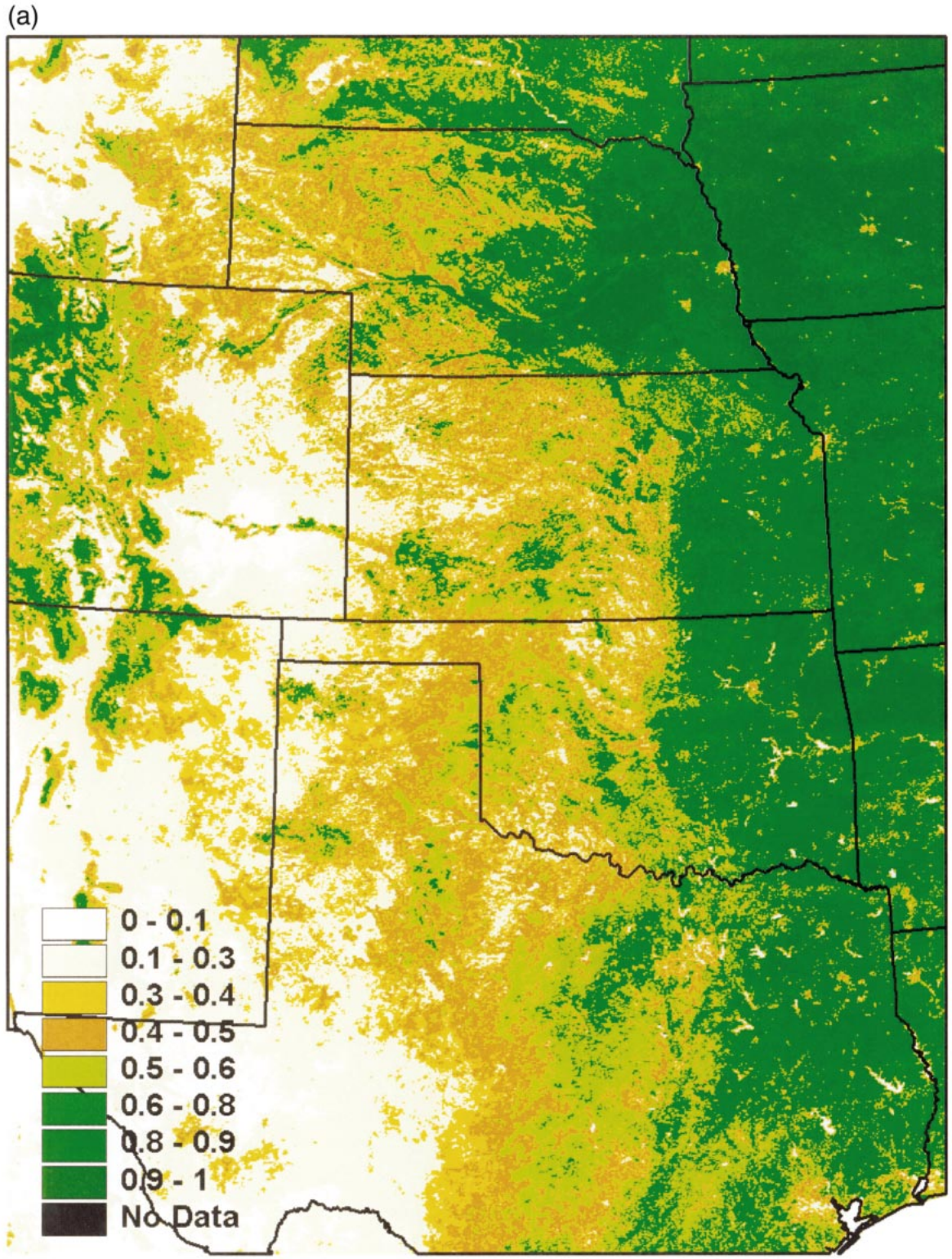

FIG. 3. Land cover parameters derived from 1-km AVHRR data from the 4–17 Jul 1997 composite: (a) fVEG, (b) albedo, and (c) LAI.

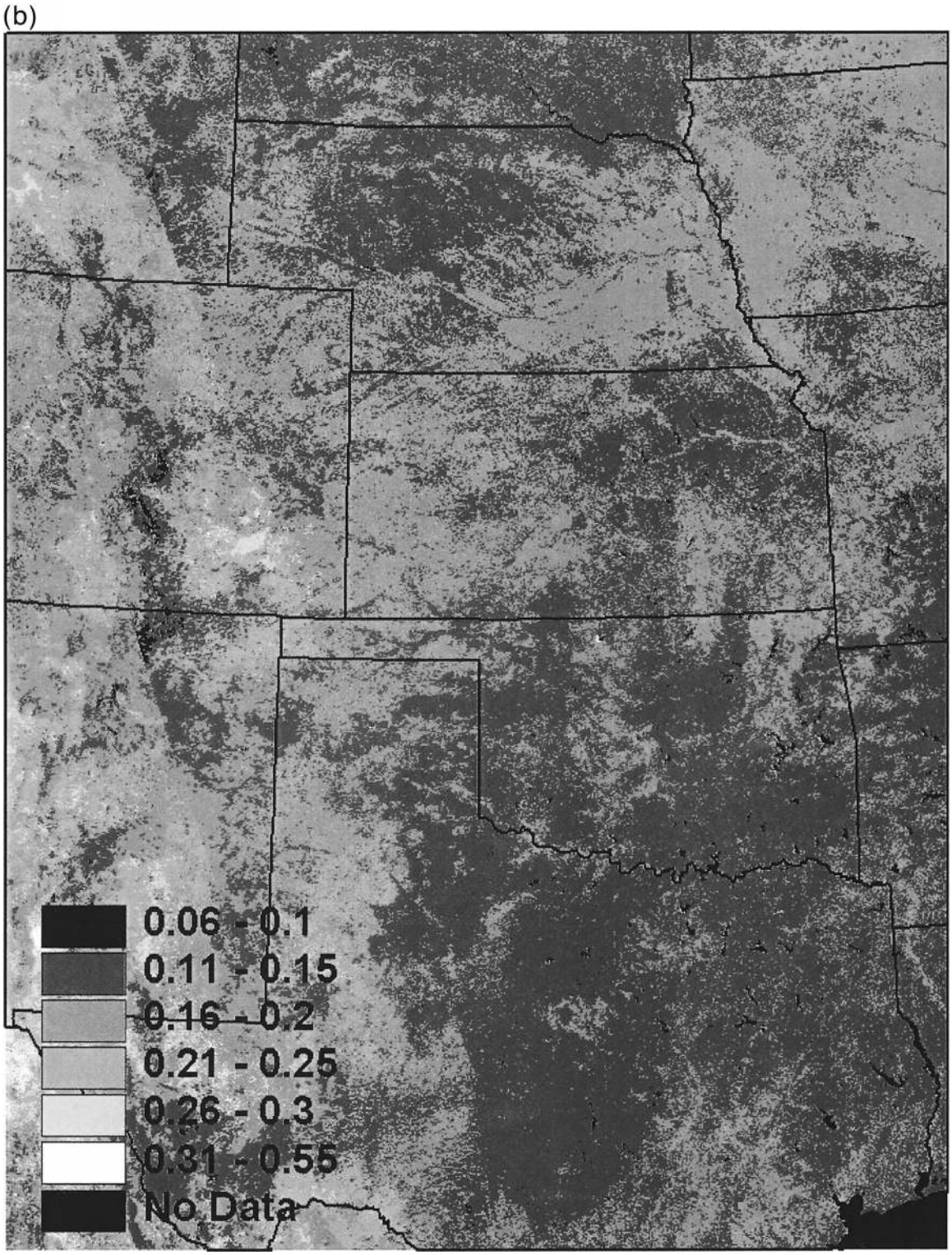

FIG. 3. (*Continued*)

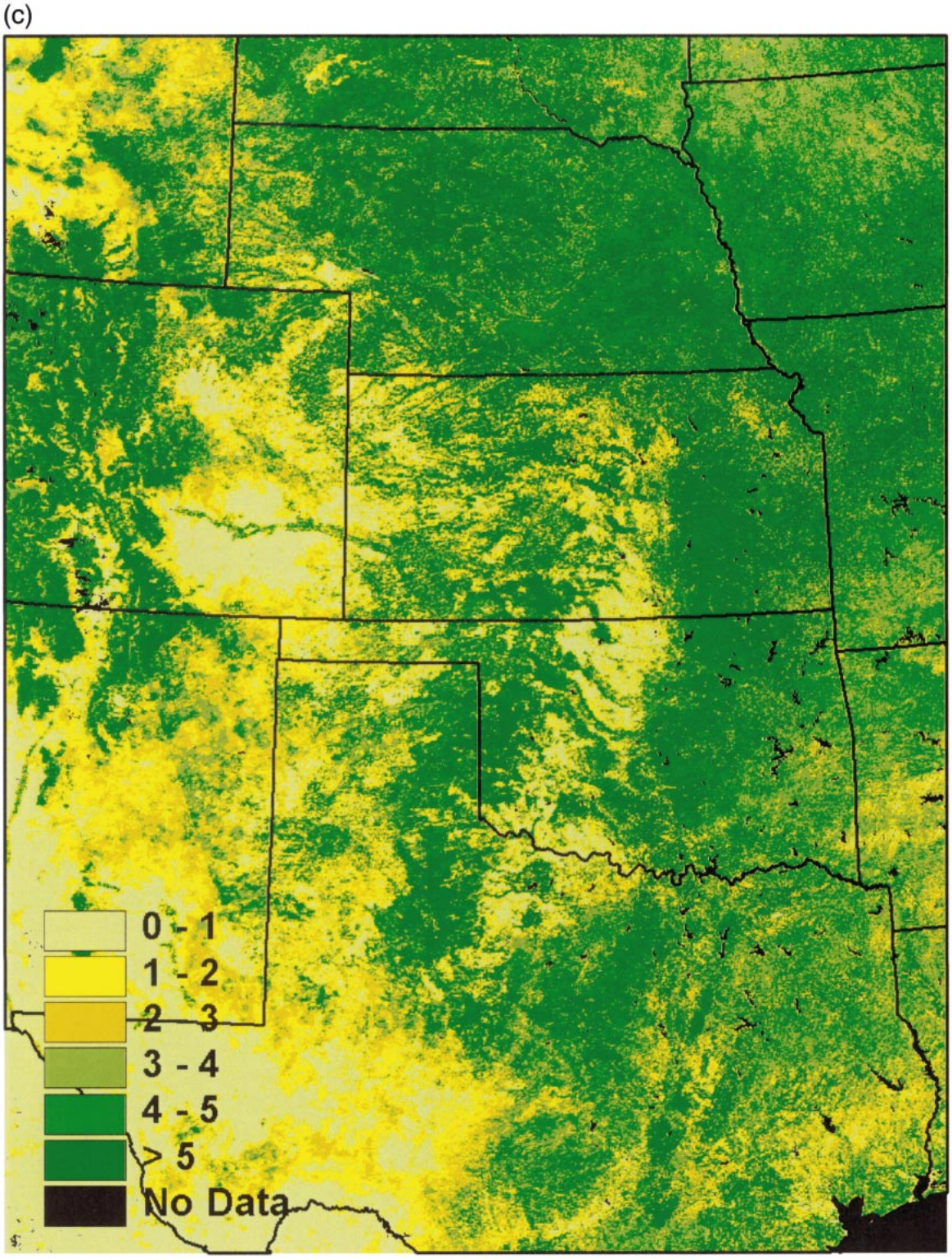

FIG. 3. (*Continued*)

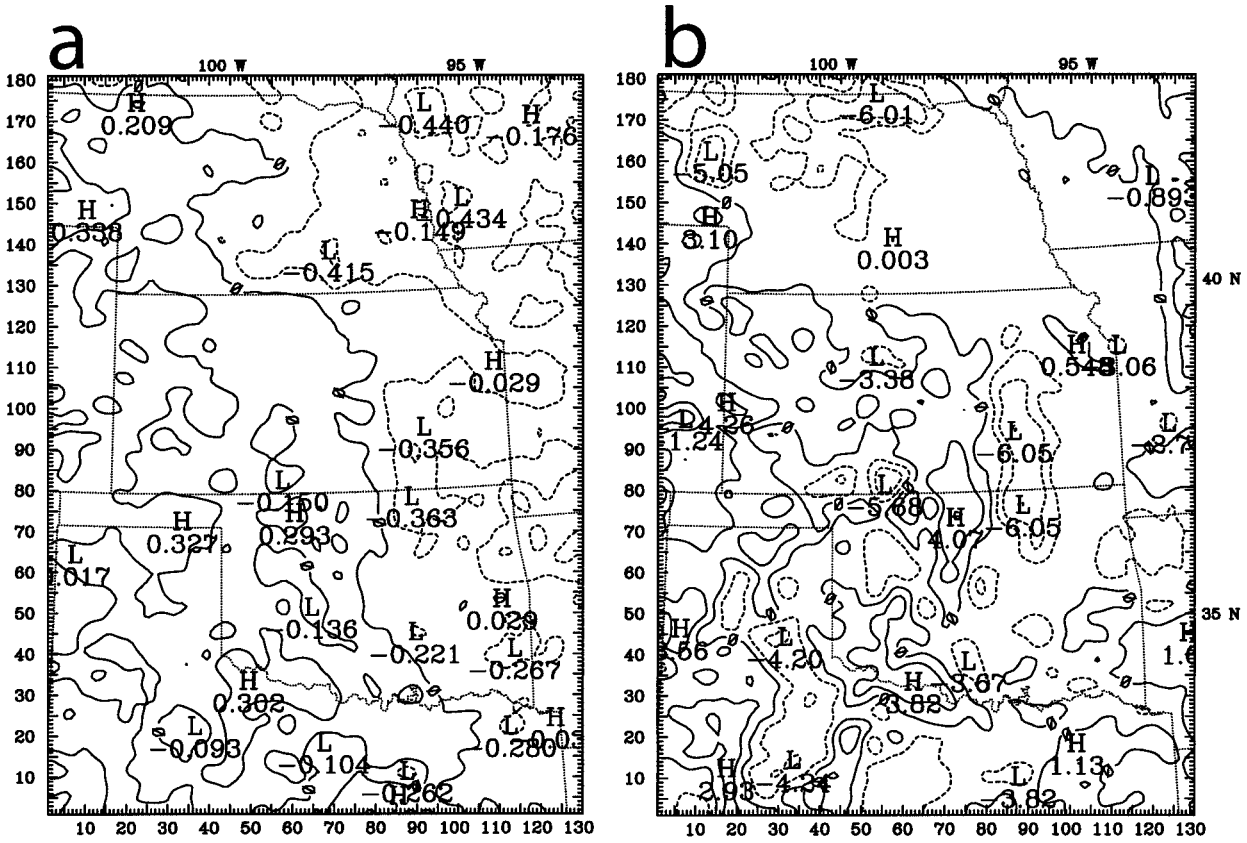

FIG. 4. Difference (ISLSCP − hi-res) fields for the parameters of (a) fVEG and (b) LAI during 4–17 Jul 1997. Contour intervals are 0.2 for fVEG and 2.0 for LAI. Plot is from the MM5 inner domain discussed in section 5.

5. Results

The model runs in this portion of the study use the same 151 × 151, 20-km grid-spacing outer domain as in section 3 but also include a 181 × 130, 6.7-km grid-spacing inner domain (see Fig. 4). The AVHRR-derived land cover data are only used on the inner grid. The model is run on each selected day from 1200 to 2100 UTC using a 35-s (11.7-s) time step on the outer (inner) domain. The atmospheric initial and boundary conditions are created as described in section 2.

Model outputs from 1500, 1800, and 2100 UTC on seven mostly clear days in July of 1997 (1, 2, 12, 25, 26, 27, and 31) are compared with temperature observations from 111 Oklahoma Mesonet sites within the inner domain at the corresponding time. The month of July is chosen because of its characteristic meteorological quiescence in Oklahoma. 2 July 1997 is studied in further detail by Mecikalski et al. (1999). To facilitate comparison, model temperatures at the lowest grid point are extrapolated downward to 1.5 m using Monin–Obukhov similarity theory. These 1.5-m gridpoint temperatures are then bilinearly interpolated to the locations of the observing stations.

Three different MM5 simulations are examined for each day: MM5 with the force–restore land surface scheme (''default''), MM5 with PLACE using the AVHRR-derived land cover data set (''hi-res''), and MM5 with PLACE using the ISLSCP monthly climatological land cover parameters (''ISLSCP''). All simulations are started using a reasonable distribution of soil moisture as determined from the calculated values of M for that day as discussed in section 2. Unless stated otherwise, the results presented are a compilation of the results from all seven days simulated.

Three statistical measures are used to compare the model simulations with observations. One measure is the Pearson (''ordinary'') correlation coefficient of linear correlation r as defined in Wilks (1995, p. 45). The second measure is the mean error, or bias, defined as

$$\text{bias} = \frac{1}{n}\sum_{i=1}^{n}(f_i - o_i), \tag{2}$$

where f_i are the forecast values, o_i are the observed values, and n is the number of observations. The last measure is rmse, defined as

$$\text{rmse} = \sqrt{\frac{1}{n}\sum_{i=1}^{n}(f_i - o_i)^2}. \tag{3}$$

Both the bias and the rmse are discussed more fully by Wilks (1995).

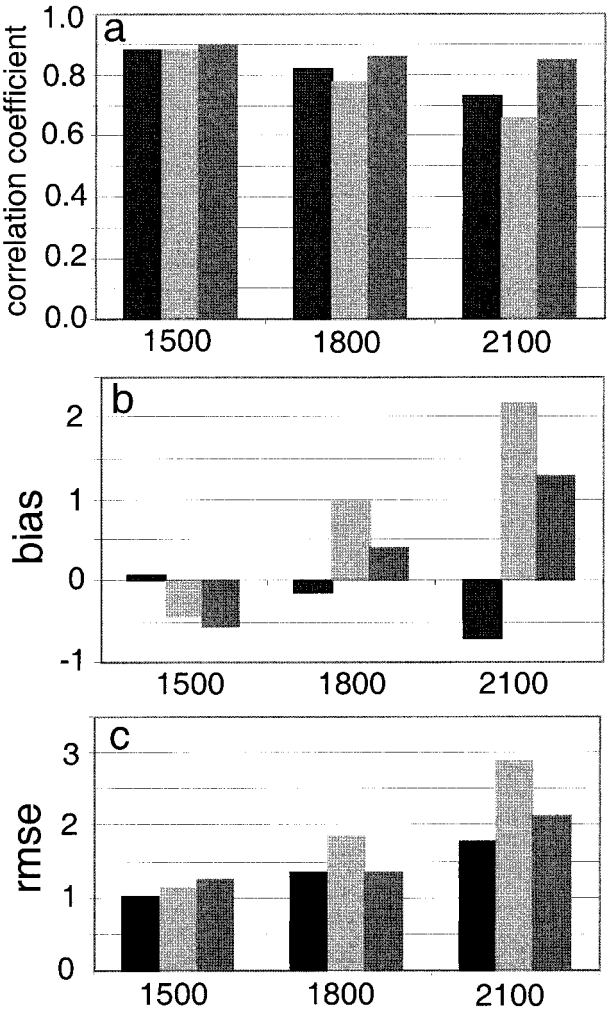

FIG. 5. Bar graphs of the mean (a) *r*, (b) bias (°C), and (c) rmse (°C) for each of the three model configurations over all seven days simulated at 1500, 1800, and 2100 UTC. Default values are in black, ISLSCP values are in light gray, and hi-res values are in dark gray.

TABLE 3. Statistics (*r*, bias, and rmse) comparing model-simulated and observed 1.5-m air temperatures at 2100 UTC during seven selected days during Jul 1997 for three different model configurations (default, ISLSCP, and hi-res). Daily statistics encompass over 190 point comparisons at both mesonet and NWS station locations across the model inner grid. The number representing the best (worst) daily performance in each of the three statistical categories is in bold (italics).

	Default *r*/bias/rmse	ISLSCP *r*/bias/rmse	Hi-res *r*/bias/rmse
1 Jul	*0.67*/−**0.21**/**2.03**	0.71/*2.94*/*3.50*	**0.78**/1.94/2.57
2 Jul	*0.84*/−**0.96**/**2.13**	0.87/*2.85*/*3.39*	**0.92**/1.64/2.18
12 Jul	0.58/−**0.15**/**1.44**	*0.57*/*2.59*/*2.98*	**0.63**/1.77/2.29
25 Jul	0.36/−**0.74**/**1.75**	*0.16*/*1.60*/*2.43*	**0.37**/1.13/1.93
26 Jul	0.23/−1.16/1.83	*0.02*/*1.69*/*2.38*	**0.35**/**1.09**/**1.73**
27 Jul	0.67/−**0.45**/**2.28**	*0.64*/*2.16*/*3.08*	**0.77**/1.60/2.47
31 Jul	**0.84**/−*0.95*/**1.43**	*0.64*/0.74/*1.82*	0.81/−**0.10**/1.48
All days	0.82/−**0.66**/**1.86**	*0.77*/*2.11*/*2.88*	**0.85**/1.28/2.12

a. Temporal changes in model temperature forecasts

The changes in model performance for each of the three configurations throughout the day show many interesting features (Fig. 5). The values of *r* between the simulated and observed temperatures decrease as the day progresses for all the configurations (Fig. 5a). This result is not surprising, given that the magnitude of the forecast errors is expected to grow as the model simulation progresses. However, the values of *r* for the hi-res runs remain high throughout the day, and the value of *r* from the hi-res run at 2100 UTC is much higher than the *r* value from the other two model runs at this time.

The bias for the default runs becomes negative during the day, implying that the modeled values of sensible heat flux are too low (Fig. 5b). On the other hand, the two PLACE configurations show a negative bias at 1500 UTC and then exhibit an increasing warm bias as the day progresses, indicative of anomalously large sensible heat flux values later in the day. The rmse values (Fig. 5c) all increase throughout the day, with the PLACE configurations showing more significant increases, especially by late in the afternoon. The largest bias and rmse values and lowest *r* values are from PLACE initialized with the land cover parameters from the ISLSCP climatological fields. The difference in the mean bias and rmse values between the ISLSCP and hi-res runs are found to be significant at the 99% level at 1800 and 2100 UTC using a Wilcoxon signed-rank test (Wilks 1995) on the 7-day mean values from each of the 111 mesonet stations. The differences between the means of the hi-res and the default runs and between the ISLSCP and the DEFAULT runs also are significant at the 99% level at these two times. The simulations valid at 2100 UTC, which act as a reasonable proxy for high-temperature forecasts, are now examined in more detail.

b. 2100 UTC

For this comparison, surface observations from NWS are also available and are added to those from the Oklahoma Mesonet, producing a total of over 190 stations within the model inner grid. Note that the results are nearly identical if either the mesonet or NWS data are used separately, so only the combined results are shown. The four highest daily values of *r* are found on 1, 2, 27, and 31 July for all three configurations (Table 3). This result implies a day-to-day variation in the quality of the model initialization. The hi-res runs produce six of the seven best daily values of *r*; the ISLSCP runs produce five of the seven worst daily values.

The magnitudes of the bias are less than 1.2°C for the default runs; larger and generally positive biases are noted for the PLACE runs (Table 3). This result suggests that the PLACE sensible heat fluxes are too large in general. The default runs have the smallest absolute bias on five of the seven days; the hi-res runs have the smallest absolute bias on the remaining two days. The rmses

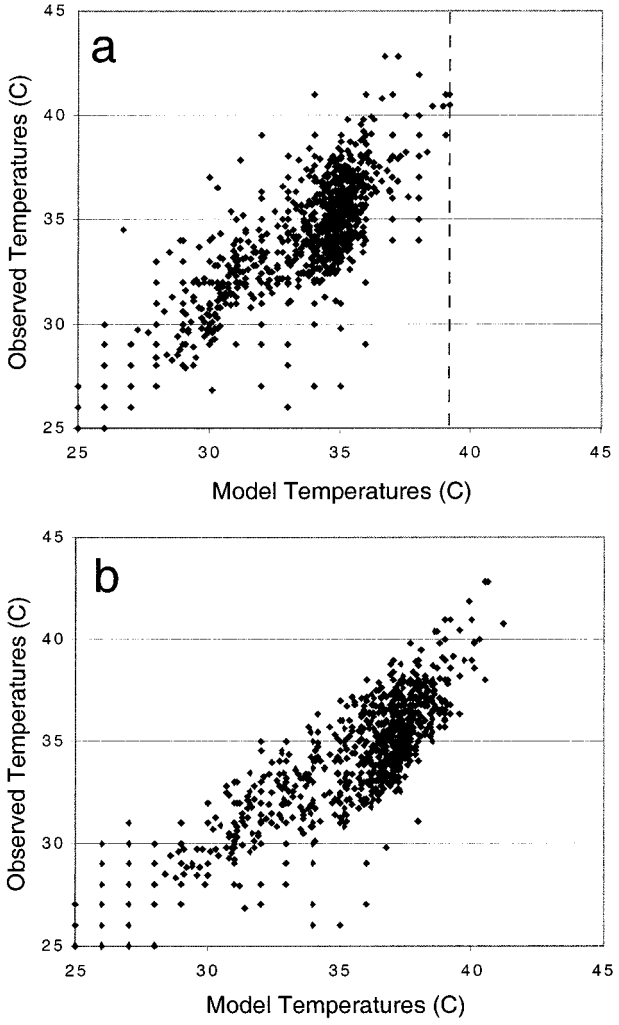

FIG. 6. Comparison of observed and modeled 2100 UTC temperatures at all 190+ stations and all 7 days (1300+ total data points) for the (a) default and (b) hi-res model configurations.

also are smaller for the default runs on six of the seven days, with the hi-res run having the smallest rmse value for 26 July.

An inspection of the monthly average values of *r*, bias, and rmse for all three configurations (last line of Table 3) shows that the default runs produce the best values of bias and rmse and the hi-res runs produce the best value of *r*. Most important, the ISLSCP land cover climatological data produce the worst values of all three average statistics and also the worst values on almost all individual days. This result clearly shows that using climatological data to specify the land cover characteristics can lead to large errors in model simulations of surface temperatures.

Mitchell et al. (2000) indicate that the operational Eta Model (Black 1994), which uses a sophisticated land surface scheme similar to that in PLACE, also has a warm bias in the north central United States during July. The Eta Model uses a 0.144° monthly fractional vegetation coverage and a 1° database for vegetation and soil types (Mitchell et al. 2000). Colby (1998) further shows that the Eta Model produces large surface temperature errors with some regularity and that the low-level temperatures from the less sophisticated Nested Grid Model are not significantly different from those of the Eta Model. Our results suggest that the surface warm bias in the Eta Model temperature forecasts may be explained in part by the use of climatological data to provide initial conditions for the land surface. These results highlight the difficulty of documenting improved simulations when comparing sophisticated land surface parameterizations with simpler land surface schemes. Without accurate information on each of the land cover parameters used by the sophisticated land surface scheme, *errors occur that may limit the gains* seen from the more sophisticated physical processes and interactions incorporated in the more complex scheme.

A comparison between the default and hi-res configurations at 2100 UTC, with points from all stations and all seven days included, shows the advantage of the default configuration in handling the low-to-moderate temperatures (Fig. 6a). In contrast, the hi-res runs display a warm bias for a majority of the data points (Fig. 6b). The total neglect of cloud cover probably contributed slightly to the warm bias, but the seven days studied were characterized by very few deviations from full insolation, so the effect is assumed to be minor. However, if only the warmest observed temperatures are analyzed (>37°C), it is apparent that the hi-res runs are significantly better than the default runs (Table 4). Temperatures from the default runs do not exceed 40°C, whereas the observations show temperatures that approach 43°C. This temperature range is reproduced much more accurately by the hi-res runs. This point is illustrated further by calculating the mean 2100 UTC temperature for each of the mesonet stations. Out of the 21 warmest mesonet stations, the hi-res runs have the lowest rmse for 15 of them.

These results suggest that the default scheme produces only moderate temperature forecasts and tends to underestimate the warmest observed temperatures. The

TABLE 4. As in Table 3, but only using data points in which the observed temperatures exceeded 37°C on all seven selected days during Jul 1997.

	Default *r*/bias/rmse	ISLSCP *r*/bias/rmse	Hi-res *r*/bias/rmse
All days ($T > 37$)	0.41/*−2.27*/*2.61*	*0.38*/0.4/1.03	**0.59**/**−0.06**/**0.99**

surprisingly good performance of the default runs may be partially attributed to the fact that July of 1997 was a fairly normal month, neither affected by drought nor excessive rainfall. It is likely that the value of hi-res runs would be further enhanced during such anomalous conditions.

6. Discussion

Results from numerical model simulations of seven days during July of 1997 clearly show the value of using satellite-derived land cover parameters as compared with model simulations that use climatological values to describe land cover characteristics. Biweekly 1-km, AVHRR-derived land cover data (LAI, fVEG, and albedo) are inserted into the model using a simple averaging technique. Temperature forecasts at 1.5 m from MM5 using a default force–restore surface energy scheme and PLACE, initialized with two different land cover datasets, are compared with observations from the Oklahoma Mesonet and NWS stations. Results from PLACE with the hi-res biweekly land cover information are significantly better than those from PLACE with monthly ISLSCP climatological land cover parameters.

Even with PLACE and the hi-res land cover parameters, however, the model simulations as a whole are considerably poorer by 2100 UTC than those for MM5 *without* PLACE. However, the hi-res runs are significantly better than the default runs at the locations with the hottest temperatures. This result indicates that the hi-res temperature simulations more accurately resolve the spatial variations in observed temperatures across the state but that a warm bias results in larger overall values of bias and rmse when using PLACE.

In this study, the sensitivity of MM5–PLACE to variations in different land cover parameters also is investigated. The proper specification of the soil moisture, LAI, and fVEG are found to be most important in providing accurate model forecasts of sensible and latent heat fluxes. For the specific case investigated, the values of LAI and fVEG are, individually, nearly as important as the soil moisture in determining the sensible heat flux. Taken together, the influence of LAI and fVEG on the partitioning of the surface energy budget is larger than the influence of soil moisture. Results also show that the surface roughness and surface albedo are of secondary importance.

It is important to emphasize that the use of PLACE with ISLSCP climatological land cover information results in significantly poorer afternoon temperature simulations than if PLACE is not used at all. Only when the 1-km, AVHRR-derived land cover parameters are implemented into PLACE do significant improvements in surface temperature simulations occur and is PLACE able to improve upon the default force–restore land surface scheme in simulating the warmest temperatures. Because Mitchell et al. (2000) show that the operational Eta Model also has a summertime warm bias similar to that found in MM5–PLACE when using the climatological land use information, it may be that an improved initialization of land surface parameters in the Eta Model will lead to smaller surface temperature forecast errors.

These results suggest that the use of satellite-derived land cover parameters will improve temperature forecasts greatly at those locations with warmest temperatures. It is expected that the greatest benefit from using such land cover data will occur during anomalous conditions when the common climatological land cover datasets have the greatest errors. As methods to detect drought-affected vegetation, the early onset of the spring green-up, regions of burned vegetation from forest fires, crop harvesting, or even long-term anthropomorphic changes in land cover improve, satellite remote sensing will become increasingly critical in temperature forecasts. The potential value of satellite-derived land cover information for model initialization is difficult to overstate.

With the recent deregulation of the power and electricity industries, an accurate high-temperature forecast can be worth hundreds of thousands or even millions of dollars on a particularly anomalous day (C. Dempsey 2000, personal communication). Results from this study show a benefit in using biweekly land cover data in a mesoscale model with a sophisticated land surface parameterization. In addition, improving the parameterization of soil moisture for model initialization is also needed (Capehart and Carlson 1994; CSCC).

Future research also needs to be directed toward enhancing methods used to derive LAI, fVEG, and albedo from AVHRR data. Improved datasets to specify other parameters for the land surface and soils are also needed. Current work includes experimentation with alternative image compositing methods designed to identify short-term land cover changes (e.g., harvesting) better and that use a new high-resolution (30 m) national land cover map derived from Landsat data (Vogelmann et al. 1998) to calibrate LAI better. In addition, alternatives for validating the land cover datasets are being explored—a problem that is very complex because of the large areal extent of the database and the frequency of observations (Merchant et al. 1994).

In February of 2000, the National Aeronautics and Space Administration began implementing the Earth Observing System (EOS). Other projects will involve testing data from the EOS Moderate-Resolution Imaging Spectroradiometer (MODIS), which will provide daily coverage of the earth in 36 spectral bands at 250–100-m resolution (Justice et al. 1998). We expect the enhanced spatial and spectral resolution afforded by MODIS to provide land cover products considerably superior to those derived from AVHRR data.

Last we wish to reinforce the notion that the incorporation of more complexity in a mesoscale numerical weather prediction model, with the intent of improving a physical parameterization, will not automatically pro-

duce better model results. Better initial data for the new parameterization may also be needed.

Acknowledgments. This study was funded by NSF Grant EPS-9871807. Thanks are extended to Yiqin Jia for providing the MM5–PLACE code and documentation. Dr. Clinton Rowe from the University of Nebraska—Lincoln provided assistance with various aspects of the remote sensing component of the project. Model initial and boundary conditions were produced at the National Center for Atmospheric Research, and the support of both NCAR/SCD and NCAR/MMM is deeply appreciated. The Pennsylvania State University–NCAR mesoscale modeling system is maintained by the efforts of many scientists at both institutions, and we are grateful for all their hard work and dedication to making this model easily accessible and user friendly. Last, the Oklahoma Climate Survey is thanked for providing the mesonet data used.

REFERENCES

Asrar, G., M. Fuchs, E. T. Kanemasu, and J. L. Hatfield, 1984: Estimating absorbed photosynthetic radiation and leaf area index from spectral reflectance in wheat. *Agron. J.,* **76,** 300–306.

Benjamin, S. G., and N. L. Seaman, 1985: A simple scheme for improved objective analysis in curved flow. *Mon. Wea. Rev.,* **113,** 1184–1198.

Black, T. L., 1994: The new NMC Mesoscale Eta Model: Description and forecast experiments. *Wea. Forecasting,* **2,** 266–278.

Blackadar, A. K., 1979: High resolution models of the planetary boundary layer. *Advances in Environmental Science and Engineering,* J. Pfafflin and E. Ziegler, Eds., Gordon and Breach, 50–85.

Box, E. O., B. N. Holben, and V. Kalb, 1989: Accuracy of the AVHRR vegetation index as a predictor of biomass, primary productivity, and net CO_2 flux. *Vegetation,* **30,** 71–89.

Brock, F. V., K. C. Crawford, R. L. Elliott, G. W. Cuperus, S. J. Stadler, H. L. Johnson, and M. D. Eilts, 1995: The Oklahoma Mesonet: A technical overview. *J. Atmos. Oceanic Technol.,* **12,** 5–19.

Brooks, H. E., and A. P. Douglas, 1998: Value of weather forecasts for electric utility load forecasting. Preprints, *16th Conf. on Weather Analysis and Forecasting,* Phoenix, AZ, Amer. Meteor. Soc., J61–J64.

Capehart, W. J., and T. N. Carlson, 1994: Estimating near-surface soil moisture availability using a meteorologically driven soil-water profile model. *J. Hydrol.,* **160,** 1–20.

Carlson, T. N., and D. A. Ripley 1990: On the relation between NDVI, fractional vegetation cover, and leaf area index. *Remote Sens. Environ.,* **62,** 241–252.

Champeaux, J.-L., D. Arcos, E. Bazile, D. Giard, J.-P. Goutorbe, F. Habets, J. Noilhan, and J.-L. Roujean, 2000: AVHRR-derived vegetation mapping over western Europe for use in numerical weather forecast models. *Int. J. Remote Sens.,* **21,** 1183–1199.

Chang, J.-T., and P. J. Wetzel, 1991: Effects of spatial variations of soil moisture and vegetation on the evolution of a prestorm environment: A numerical case study. *Mon. Wea. Rev.,* **119,** 1368–1390.

Chen, F., and Coauthors, 1996: Modeling of land-surface evaporation by four schemes and comparison with FIFE observations. *J. Geophys. Res.,* **101,** 7251–7268.

Chen, T. H., A. Henderson-Sellers, P. C. Milly, A. J. Pitman, and A. C. Beljaars, 1997: Cabauw experimental results from the Project for Intercomparison of Land-Surface Parameterization Schemes. *J. Climate,* **10,** 1194–1215.

Colby, F. P., Jr., 1998: A preliminary investigation of temperature errors in operational forecasting models. *Wea. Forecasting,* **13,** 187–205.

Collins, D. C., and R. Avissar, 1994: An evaluation with the Fourier amplitude sensitivity test (FAST) of which land-surface parameters are of greatest importance in atmospheric modeling. *J. Climate,* **7,** 681–703.

Crawford, T. M., D. J. Stensrud, T. N. Carlson, and W. J. Capehart, 2000: Using a soil hydrology model to obtain regionally averaged soil moisture values. *J. Hydrometeor.,* **1,** 353–363.

Csiszar, I., and G. Gutman, 1999: Mapping global land surface albedo from NOAA AVHRR. *J. Geophys. Res.,* **104,** 6215–6228.

Deardorff, J. W., 1978: Efficient prediction of ground surface temperature and moisture, with inclusion of a layer of vegetation. *J. Geophys. Res.,* **83,** 1889–1903.

Dempsey, C. L., K. W. Howard, R. A. Maddox, and D. H. Phillips, 1998: Developing advanced weather technologies for the power industry. *Bull. Amer. Meteor. Soc.,* **79,** 1019–1035.

Dickinson, R. E., and A. Henderson-Sellers, 1988: Modeling tropical deforestation: A study of GCM land-surface parameterizations. *Quart. J. Roy. Meteor. Soc.,* **114,** 439–462.

——, ——, P. J. Kennedy, and M. F. Wilson, 1986: Biosphere-Atmosphere Transfer Scheme (BATS) for the NCAR Community Climate Model. NCAR Tech. Note NCAR/TN-275+STR, 69 pp.

Dudhia, J., 1993: A nonhydrostatic version of the Penn State–NCAR Mesoscale Model: Validation tests and simulation of an Atlantic cyclone and cold front. *Mon. Wea. Rev.,* **121,** 1493–1513.

Ehrlich, D., J. E. Estes, and A. Singh, 1994: Applications of NOAA-AVHRR 1 km data for environmental monitoring. *Int. J. Remote Sens.,* **15,** 145–161.

Eidenshink, J. C., and J. A. Hutchinson, 1993: AVHRR data set for the conterminous United States. *Res. Explor.,* **Water Issue,** 86–97.

Emanuel, K. A., and Coauthors, 1995: Report of the First Prospectus Development Team of the U.S. Weather Research Program to NOAA and the NSF. *Bull. Amer. Meteor. Soc.,* **76,** 1194–1208.

Gutman, G., and A. Ignatov, 1995: Global land monitoring from AVHRR: Potential and limitations. *Int. J. Remote Sens.,* **16,** 2301–2309.

——, and ——, 1998: The derivation of the green vegetation fraction from NOAA/AVHRR data for use in numerical weather prediction models. *Int. J. Remote Sens.,* **19,** 1533–1543.

Justice, C. O., and Coauthors, 1998: The moderate resolution imaging spectroradiometer (MODIS): Land remote sensing for global change research. *IEEE Trans. Geosci. Remote Sens.,* **36,** 1228–1249.

Lawford, R. G., 1999: A midterm report on the GEWEX Continental-Scale International Project (GCIP). *J. Geophys. Res.,* **104,** 19 279–19 292.

Los, S. O., and Coauthors, 2000: A global 9-year biophysical land-surface dataset from NOAA AVHRR data. *J. Hydrometeor.,* **1,** 183–199.

Loveland, T. R., J. W. Merchant, J. F. Brown, D. O. Ohlen, B. Reed, and P. Olsen, 1995: Seasonal land cover regions of the United States. *Ann. Assoc. Amer. Geogr.,* **85,** 339–355.

Mecikalski, J. R., G. R. Diak, M. C. Anderson, and J. M. Norman, 1999: Estimating fluxes on continental scales using remotely sensed data in an atmospheric–land exchange model. *J. Appl. Meteor.,* **38,** 1352–1369.

Merchant, J. W., L. Yang, and W. Yang, 1994: Validation of continental-scale land cover databases derived from AVHRR data. *Proc. Pecora 12 Symp.,* Bethesda, MD, Amer. Soc. Photogr. Remote Sens., 63–72.

Mitchell, K., and Coauthors, 2000: Recent GCIP-sponsored advancements in coupled land-surface modeling and data assimilation in the NCEP Eta Mesoscale Model. Preprints, *15th Conf. on Hydrology,* Long Beach, CA, Amer. Meteor. Soc., 180–183.

Monteith, J. L., and M. H. Unsworth, 1990: *Principles of Environmental Physics.* Edward Arnold, 291 pp.

National Research Council, 1991: *Opportunities in the Hydrologic Sciences.* National Academy Press, 368 pp.

Niyogi, D. S., S. Raman, and K. Alapaty, 1999: Uncertainty in the specification of surface characteristics, part II: Hierarchy of interaction-explicit statistical analysis. *Bound.-Layer Meteor.,* **91,** 341–366.

Noilhan, J., and S. Planton, 1989: A simple parameterization of land surface processes for meteorological models. *Mon. Wea. Rev.,* **117,** 536–549.

Pitman, A., R. Pielke, R. Avissar, M. Claussen, J. Gash, and H. Dolman, 1999: The role of land surface in weather and climate: Does the land surface matter? *IGBP Newsletter,* Vol. 39, 4–11.

Price, J. C., 1993: Estimating leaf area index from satellite data. *IEEE Trans. Geosci. Remote Sens.,* **31,** 727–734.

Rabin, R. M., S. Stadler, P. J. Wetzel, D. J. Stensrud, and M. Gregory, 1990: Observed effects of landscape variability on convective clouds. *Bull. Amer. Meteor. Soc.,* **71,** 272–280.

Reed, B. C., and L. Yang, 1997: Seasonal vegetation characteristics of the United States. *GeoCarto,* **12,** 65–71.

Schwartz, M. D., and T. R. Karl, 1990: Spring phenology: Nature's experiment to detect the effect of ''green-up'' on surface maximum temperatures. *Mon. Wea. Rev.,* **118,** 883–890.

Sellers, P. J., and Coauthors, 1995: Remote sensing of the land surface for studies of global change: Models–algorithms–experiments. *Remote Sens. Environ.,* **51,** 3–26.

——, and Coauthors, 1996: The ISLSCP Initiative I global datasets: Surface boundary conditions and atmospheric forcings for land–atmosphere studies. *Bull. Amer. Meteor. Soc.,* **77,** 1987–2005.

Sud, Y. C., J. Shukla, and Y. Mintz, 1988: Influence of land surface roughness on atmospheric circulation and precipitation: A sensitivity study with a general circulation model. *J. Appl. Meteor.,* **27,** 1036–1054.

Vogelmann, J. E., T. Sohl, and S. M. Howard, 1998: Regional characterization of land cover using multiple sources of data. *Photogr. Eng. Remote Sens.,* **64,** 45–57.

Wetzel, P. J., and J.-T. Chang, 1988: Evapotranspiration from nonuniform surfaces: A first approach for short-term numerical weather prediction. *Mon. Wea. Rev.,* **116,** 600–621.

——, and A. Boone, 1995: A parameterization for land–atmosphere–cloud exchange (PLACE): Documentation and testing of a detailed process model of the partly cloudy boundary layer over heterogeneous land. *J. Climate,* **8,** 1810–1837.

——, D. Atlas, and R. H. Woodward, 1984: Determining soil moisture from geosynchronous satellite infrared data: A feasibility study. *J. Climate Appl. Meteor.,* **23,** 375–391.

Wilks, D. S., 1995: *Statistical Methods in the Atmospheric Sciences.* Academic Press, 467 pp.

——, 1997: Forecast value: Prescriptive decision studies. *Economic Value of Weather and Climate Forecasts,* R. W. Katz and A. H. Murphy, Eds., Cambridge University Press, 109–145.

Wydick, J. E., P. A. Davies, and A. Gruber, 1987: Estimation of broadband planetary albedo from operational narrowband satellite measurements. NOAA Tech. Rep. NESDIS 27, 32 pp.

Yin, Z., and T. H. L. Williams, 1997: Obtaining spatial and temporal vegetation data from Landsat MSS and AVHRR/NOAA satellite images for a hydrologic model. *Photogr. Eng. Remote Sens.,* **63,** 69–77.

Zhang, D., and R. A. Anthes, 1982: A high resolution model of the planetary boundary layer—sensitivity tests and comparisons with SESAME-79 data. *J. Appl. Meteor.,* **21,** 1594–1609.

Zhangshi, Y., and T. H. L. Williams, 1997: Obtaining spatial and temporal vegetation data from Landsat MSS and AVHRR/NOAA satellite images for a hydrological model. *Photogr. Eng. Remote Sens.,* **63,** 69–77.